MAGNETIC MATERIALS THIN FILMS AND PARTICLES

1. Introduction

The largest use of magnetic films and particles, in the form of tapes and disks for recording and retention of audio, visual, and digital information, is in memory and storage technologies (see INFORMATION STORAGE MATERIALS, MAGNETIC). Price per bit of information, including the cost of the peripheral electronics, and performance, as denoted by access time, generally are used to characterize the various memory technologies. Power, modular capacity, reliability, nonvolatility, etc, are also factors describing the efficacy of memories.

2. Magnetic Properties and Structure

The static or low frequency magnetic properties pertinent to thin-film materials generally are utilized to characterize magnetic materials. As a first approximation, these properties serve to suggest utility for device applications. Saturation magnetization M_s and Curie temperature T_C are intrinsic (structure insensitive) properties and are equal to the bulk values when thick films are made properly. For very thin highly paramagnetic films, such as those of platinum, sandwiched between ferromagnetic, eg, Co, or antiferromagnetic, eg, Cr, thin films, in the form of multilayered structures being developed for recording heads, a magnetization can be induced in the normally paramagnetic material (see MAGNETIC MATERIALS, BULK). The surface area-to-volume ratio of the individual layers is so large that the atomic moments at the interfaces play an important role.

The extrinsic or structure-sensitive properties depend on size, shape, and surface topography of the films; the size, shape, and orientation of crystallites in polycrystalline films; concentration and distribution of imperfections, impurities, and alloying elements; and state of residual stress. The extrinsic properties can be classified further as static or dynamic depending on whether or not the property displays a frequency dependence. Remanent magnetic induction, B_r; coercive force, H_c; and permeability, μ, are examples of static extrinsic properties. Eddy-current loss and resonance of spins and domain walls typify structure-sensitive dynamic properties. However, high frequency dynamic measurements generally are required for final evaluation of magnetic films. Thin-film preparation techniques, such as the deposition process employed, also highly influence magnetic properties (see THIN FILMS).

Shape anisotropy generally causes the magnetization M_s in thin films to be in the plane of the film. Otherwise a huge demagnetizing field $H_d(=4\pi M_s)$ would act normal to the plane of the film if M_s were turned in that direction. Similarly, the magnetization in rod-like acicular particles of large aspect ratios may prefer to lie in the long direction. Domains in the films extend completely through the film thickness, and the walls between them are largely 180° and roughly parallel to the easy axis of the film. If the magnetization vector rotates about the wall normals, the walls are called Bloch walls and result in free poles

existing on the surface. Bloch walls can exist in bulk materials. For very thin films, eg, ca 50 nm and less, the magnetostatic energy can be reduced if the magnetization vector forming the 180° wall rotates about the film normal. This wall is a Néel wall and free poles do not exist on the surface. Cross-tie walls also can exist in very thin films. A cross-tie wall is crossed at regular intervals by Néel-wall segments and its energy is less than both a Bloch wall and Néel wall in a certain range of film thicknesses. In general, films of technological interest are of such thickness that only Bloch walls are stable. A detailed discussion of domain walls in films and magnetization dynamics is available (1).

In addition to shape anisotropy, an induced anisotropy represented by the constant K_u can be present in films as a result of deposition in a magnetic field. These anisotropies result from short-range directional order or an anisotropic distribution of atom pairs. In the liquid-phase epitaxy (LPE) of single-crystal, mixed-garnet films, the uniaxial anisotropy also appears to be a result of short-range order resulting from the growth process. The induced anisotropy constant is related to the anisotropy field H_k, where $H_k = 2K_u/M_s$. H_k is the field required to rotate the magnetization from the easy axis into the hard directions.

In a polycrystalline film, the easy axis can vary from point to point about an average direction. This dispersion is represented by a dispersion angle, α, which is the dispersion of easy axes about the average direction. A film quality factor q, where $q = H_c/\alpha H_k$, is used as a measure of the usefulness of a material for device applications. It is desirable to maximize this ratio: higher H_c helps make the material more resistant to stray fields, and αH_k determines the drive currents for maximum output (2, 3). The effects of all of the deposition variables on the structure and magnetic properties of films are discussed in the literature (3–9).

Permalloys, eg, 81.5% Ni–18.5% Fe, exhibit very low magnetocrystalline anisotropy and magnetostriction. Very low or zero magnetostriction is necessary for storage elements because dimensional changes, which can lead to stresses, are absent when the magnetization is switched. Substrate temperature and deposition rate influence the kinetics of film growth, the degree of impurity incorporation, and the residual stress distribution. For evaporated Permalloy films, H_c remains essentially constant up to a substrate temperature of ca 425°C; then H_c rises rapidly (6). Smaller deposition rates result in lower H_c and H_k for a given substrate temperature, although the deposition rate least affects H_c. Grain size increases with substrate temperature. H_k is affected markedly by the angle at which the metal atoms strike the substrate at low (<300°C) deposition temperatures, because the grains or crystallites are no longer equiaxed but elongated. Easy axis dispersion is relatively independent of rate or temperature up to ca 400°C and then increases sharply.

Sputtering offers advantages over vacuum evaporation. Using sputtering techniques, angle of incidence effects are absent, film composition is generally the same as target composition, and melt composition need not be periodically altered. Additionally deposition rate and film thickness are easily controlled. The effect of argon pressure and sputtering-power density on coercivity and magnetoresistance of 500-nm 80.6 wt % Ni–19.4 wt % Fe films has been studied (7), and the results are shown in Figure 1. Magnetoresistance behavior of Permalloy films is important because these are used for detection in bubble memory devices.

As shown in Figure 1**a**, resistivity and coercivity decrease with increasing sputtering-power density, whereas the magnetoresistance coefficient increases. The magnetoresistance coefficient is defined as $\Delta R(100)/R_o$, where R_o is the electrical resistance when current flows parallel to the magnetic easy axis and ΔR is the change of R_o in a field of 15.92 A/cm (20 Oe) applied perpendicular to the current flow. At constant power density, maximum magnetoresistance and minimum coercivity are obtained at lower argon pressure (Fig. 1**b**). Films that are sputtered at lower power density (low deposition rate) contain more trapped impurities, eg, O_2 and N_2, from the Ar and from the chamber walls which account for the higher coercivity and zero field resistances. At lower Ar pressures, there are decreased deposition rates and fewer impurity atoms striking the film surface (see THIN FILMS, FORMATION TECHNIQUES).

The effect of applying a 100 V negative bias voltage relative to the anode is shown in Table 1 (8). H_c and H_k are independent of deposition rate if a negative bias voltage is applied. Also, large amounts of oxygen or nitrogen impurities in the film are tolerated before magnetic properties deteriorate.

3. Fabrication

3.1. Thermal Evaporation. Thermal evaporation in vacuum, the oldest and most economical method of thin-film preparation, is illustrated in Figure 2**a** and consists of heating the material that is to be deposited to a temperature at which appreciable vapor pressure is developed. The vapor condenses onto an appropriately placed substrate which may be maintained at any temperature. Heating of the evaporant is accomplished either by use of a resistance heater or by an electron beam. Electron-beam heating is preferred because higher melting metals can be evaporated without contamination, as occurs in crucibles. Water-cooled copper crucibles can be used, and multiple heaters can be used for deposition of alloys. Flash evaporation, a technique for evaporating an alloy where the constituents differ widely in vapor pressure, can be performed by placing a small amount of the evaporant on a very hot source where all of the evaporant flash evaporates. Ion plating is a variant of evaporation in which a high d-c or r-f voltage is used to ionize the evaporant and accelerate it onto the substrate. The substrate, which is the cathode, is in a high voltage gas discharge. Discussions of crucible materials that are used for supporting various evaporants, heaters, the cosine law of emission, film thickness measurement, and thickness distribution of evaporated films are included in Reference 9.

3.2. Sputtering. Cathodic sputtering processes have come into widespread production use. As schematically illustrated in Figure 2**b**, material is sputtered from a source target (cathode) by inert (argon) energetic ions and deposits on a substrate (anode). The glow discharge may be produced either by a d-c voltage (d-c sputtering) or under r-f conditions. The r-f diode is the most widely used. It permits sputtering of nonconducting or dielectric materials, is characterized by high deposition rates, can be scaled up to handle large substrate loads, the substrates can be sputter-etched clean prior to deposition, and the diode can be operated in a bias-sputtering mode. Another advantage of

the sputtering process is that materials of low or zero vapor pressure can be deposited in thin-film form.

A primary source of substrate heating during sputtering is electron bombardment of secondary electrons produced by ion bombardment of the cathode. The secondary electrons can depress the deposition rates by biasing the substrate (anode) negatively, resulting in resputtering of the deposit by Ar ions. However, this problem is not encountered with ion-beam sputtering. The ion beam, which is generated from a separate source, strikes the target in the deposition chamber and the sputtered target atoms are deposited on a substrate in front of the target (10).

3.3. Magnetron Sputtering. In magnetron sputtering the discharge is contained near the anode and cathode. This type of sputtering results in high deposition rates, and low substrate heating. It is particularly important where sputtering is carried out at low Ar pressures, eg, ca 2.7 Pa (2.0×10^{-2} mm Hg), so as to minimize the effects of higher Ar pressures, such as gas entrapment in the film. The higher deposition rate results from increased ionizing efficiency caused by the magnetic field. The magnetic field increases the path length of the ionizing electrons. Another method of increasing sputtering rates at lower Ar pressures is by triode sputtering by which an increased quantity of ionizing electrons is supplied thermionically from a filament.

In reactive sputtering, the evaporant in the glow discharge is exposed to reactive gases, eg, oxygen. Reactive sputtering is used for depositing hard-to-form deposits, for example, oxide dielectrics, when starting with a metallic alloy target.

Minimization of contamination of the sputtered film by reactive residual gases, eg, O_2, N_2, H_2O, hydrocarbons, etc, in the system can be accomplished by bias sputtering (11) and getter sputtering (12). In the former process, a small negative bias is applied to the substrate or film being deposited by d-c sputtering. The reduced contamination appears to be a result of positive-ion bombardment of the film during deposition, and adsorbed gases, which could be trapped as impurities, are sputtered off. In a-c sputtering, the cathode and anode are bombarded alternately by ions. In the latter process, sputtering is confined within an anode can surrounding the cathode and anode and a portion of the sputtered material is used to purify or getter the argon before it reaches that part of the system where deposition occurs. Detailed discussions of cathode and r-f sputtering are given in References (13–15).

Off-Axis Magnetron Sputtering. When the substrate faces the target, the technique is referred to as on-axis sputtering. This technique gives the fastest film growth rate. However, this arrangement and low pressures generally yield poor quality films, particularly in terms of stoichiometry and defects for multicomponent materials. The off-axis geometry, schematically shown on Figure 3**a**, overcomes these problems and has been used to make high quality high temperature ternary superconducting oxide films. The substrates are also mounted on a heater–holder which is outside the region of direct on-axis ion flux but still within the outer edge of the plasma region. The atoms that deposit on the substrate are generally low energy thermalized neutral atoms and the film stoichiometry matches the target. The off-axis arrangement convenient for the preparation of multilayer magnetic structures is shown in Figure3**b**.

3.4. Pulsed Laser Evaporation. Laser evaporation or ablation consists of using a laser emitting at an appropriate wavelength, generally a KrF excimer laser, in a pulsed mode in a controlled atmosphere to deposit a thin film of a material the composition of which is that of the target (16–18) (see LASERS). The process can be modified to carry out plasma-assisted laser deposition by placing a bias voltage between a grid and the source. The role of the plasma is to enhance the chemical reactions leading to the formation of the film and to modify the growth and hence the properties of the film (see PLASMA TECHNOLOGY). Films of the high temperature oxide superconductors and dielectric and optical materials, for example $LiNbO_3$ and $Ba_{0.5}Sr_{0.5}TiO_3$, have been deposited on sapphire (α-Al_2O_3) and silicon.

3.5. Molecular Beam Epitaxy. Molecular beam epitaxy (MBE), a high vacuum process for producing high quality ultrathin single-crystal layers, was initially developed for the production of multilayer thin film semiconductor devices based on gallium arsenide, GaAs (19). The sources for the atomic beams of Group 3 (III) to Group 15 (V) elements were condensed phases of the elements located in effusion ovens (Fig. 4). Subsequently, the process was successfully extended to the use of gas-phase sources (20) which gave higher quality GaAs and indium phosphide, InP, films. Metal organic chemical vapor deposition (MOCVD) is a cold-wall process which utilizes volatile metal organic compounds, as sources for the Group 3 (III) to Group 15 (V) elements (21–23). These processes are under investigation for the preparation of Group (III) to (V) semiconductor films having magnetic materials.

3.6. Chemical Vapor Deposition. In chemical vapor deposition (CVD), often referred to as vapor transport, the desired constituent(s) to be deposited are in the form of a compound existing as a vapor at an appropriate temperature. This vapor decomposes with or without a reducing or oxidizing agent at the substrate–vapor interface for film growth. CVD has been used successfully for preparing garnet and orthoferrite films (24,25). Laser-assisted CVD is also practiced.

3.7. Electrolytic and Electroless Deposition. In electrodeposition, the substrate to be coated is the cathode of an electrolytic cell and the element(s) to be formed into a film are present as ions in an appropriate electrolyte (plating bath) which is in contact with the substrate. By application of an external voltage, the ions are reduced at the substrate surface, thereby forming the film. The quality of the film surface and composition, important in determining the intrinsic and extrinsic magnetic properties, is influenced greatly, among other things, by the external voltage, bath composition, nature of the anode, surface topography of the film, metallurgical structure, ie, grain size, etc, and cleanliness of substrate surface. Historically the largest application of electrodeposition in producing magnetic films was for plated-wire memories using Permalloy. However, the advent of larger capacity memories such as magnetic tape and disk, compact disk-read only, and semiconductor, has resulted in diminished importance of plated-wire memory, as well as planar memory, technology. Comprehensive discussions of electrodeposition of Permalloy films, influence of film structure on magnetic behavior, and plated-wire memories may be found in the literature (26–28).

In electroless deposition, the substrate, prepared in the same manner as in electroplating (qv), is immersed in a solution containing the desired film components (see ELECTROLESS PLATING). The solutions generally used contain soluble nickel salts, hypophosphite, and organic compounds, and plating occurs by a spontaneous reduction of the metal ions by the hypophosphite at the substrate surface, which is presumed to catalyze the oxidation–reduction reaction.

3.8. Growth from Solution. In solution growth, film growth is accomplished by immersing the substrate in a saturated or supersaturated solution containing the film constituents. If the solution is saturated initially, the temperature is lowered after immersion to a temperature at which it becomes supersaturated. Film growth then occurs by precipitation onto the substrate surface. If the solution is supersaturated initially, spontaneous growth occurs very soon after the substrate is immersed and film growth occurs at constant temperature until the solution becomes saturated at that temperature. If the substrate is a single-crystal slice and the film is to be a single crystal of identical crystal orientation as the substrate, the process is liquid-phase epitaxy (LPE).

Liquid-Phase Epitaxy. The LPE process (29), which was applied first to the preparation of semiconductor devices, is the growth process that was used for producing bubble memories based on magnetic garnets. The oxide components for the garnet film were dissolved in a molten oxide flux, eg, $PbO–B_2O_3$, contained in a Pt crucible, and the single-crystal, nonmagnetic garnet slice, generally gadolinium gallium garnet (GGG) immersed into the solution for film growth. Bubble memories are no longer produced.

4. Materials

Magnetic storage materials for storage of audio and video information as well as of digital data are in the form of tape and disks. Optical disks for data storage came into use in 1985; magnetooptic recording systems were being produced as of 1994. Recording materials, which generally exhibit coercivities in the range of 25–100 kA/m (300–1250 Oe), can be classified as semihard.

There are two states of remanent magnetization for recording: longitudinal, in which the magnetization is in the plane of the recording medium; and perpendicular, in which the magnetization is normal to the plane. For particulate media in which the acicular submicronic particles are single domain and embedded in plastic, the magnetization is confined in the direction of the long dimension. The length-to-width ratios are of the order of 5 to 1, with the long dimension approximately 1 μm. Subsequent recording applications led to the development of thin-film metallic coatings so as to achieve higher saturation magnetization and recording density and the ability to tailor, by alloying, the desired magnetic properties.

Multilayer materials exhibiting high magnetization and permeability are undergoing considerable research and development for advanced recording heads. The discovery of giant magnetoresistance in multilayered nano-thick magnetic materials is expected to become important for advanced read heads. Newer magnetooptical materials have the potential for increased storage density

in magnetooptical recording. Magnetic and magnetooptic storage technology has been identified as one of the 22 critical technologies for the United States.

4.1. Particulate Materials. There are three principal classes of particulate magnetic materials: γ-ferric oxide, γ-Fe_2O_3, and its modifications; chromium dioxide [12018-01-8], CrO_2; and iron [7439-89-6]. A comparison of the remanent magnetization, B_r, and coercivity, H_c, for several γ-Fe_2O_3 material systems in commercial use or for those being commercialized, ie, barium ferrite [11138-11-7], $BaFe_{12}O_{19}$, is shown in Table 2. γ-Fe_2O_3, the most popular magnetic tape material, is used for general-purpose audio recording. Fe_3O_4 has been used instead of γ-Fe_2O_3 for tape. As can be seen from the table, solid solutions of γ-Fe_2O_3 and Fe_3O_4 result in increased H_c. γ-Fe_2O_3 containing Co exhibits even higher coercivities. CrO_2 containing a few percent of Co also results in increased coercivity. Although acicular particles of metals can be produced, problems of chemical stability such as resistance to oxidation, and production costs have prevented use in large amounts in recording media.

A larger B_r leads to heightened readout amplitude, whereas the larger coercive force and thinner film lead to greater recording density. Considerable progress has been made in increasing packing density, uniaxial behavior (acicularity), and homogeneity in size distribution of the γ-Fe_2O_3 particles, as well as attaining higher coercivities. Higher packing densities result in larger output signals at all frequencies. Homogeneity in shape and size results in higher squareness ratios (B_r/B_s) and in homogeneity in particle-switching fields. Higher coercivities are required for higher frequency operation and are a result of increased uniaxial anisotropy through shape and magnetocrystalline anisotropies.

One of the early problems associated with the development of CrO_2 for tape was its chemical instability in organic binders. The stability of CrO_2 particles has been enhanced by the use of a surface-reduction treatment, and high coercivity CrO_2 is available for high quality video tape. The beneficial effect of Co in increasing the coercivity of γ-Fe_2O_3 has been exploited in Japan where the deleterious effects of Co resulting from increased magnetoresistive and anisotropy changes have been minimized through preparation of surface-modified γ-Fe_2O_3, ie, formation of a thin surface layer of cobalt ferrite [12052-28-7], $CoFe_2O_4$, on γ-Fe_2O_3 particles (30).

4.2. Recording Heads. Materials that are suitable for read/write recording heads for tapes and disks are characterized by high saturation flux density, low remanent induction to avoid erasure of information when the writing current ceases, and low hysteresis and low eddy-current loss, particularly for high data rates or high frequency operation. In addition, because of the small air gap between the head and recording medium, the head material should be abrasion resistant. Dust particles and the magnetic attraction between head and tape can lead to abrasion.

The early recording heads were based on bulk Ni–Fe permalloy and manganese–zinc ferrite, which are soft magnetic materials (see FERRITES). For general-purpose audio recording, laminated Ni–Fe alloys exhibit the required high saturation and low remanence and eddy-current losses; moreover, abrasion is low. Head wear is improved by use of precipitation hardened material. The spinel structure oxides, manganese–zinc and nickel–zinc ferrites, exhibit good

abrasion resistance and high frequency characteristics and in some cases are the preferred material despite their relatively low saturation.

For high quality audio and video recording where the recording medium is CrO_2 or Co impregnated γ-Fe_2O_3, sputtered Sendust alloy films (9.6 wt% Si, 5.4 wt% Al, balance Fe; see also Table 3) and ferrites are used as head materials. Sendust exhibits nearly the same resistivity as the ferrites, but the films of this material exhibit higher (1.1 T (11 kG)) saturation flux densities and effective permeabilities of 240 at 20 MHz. Wear resistance is also very good. Ni–Zn and Mn–Zn ferrites are generally used in video and high frequency recording because eddy currents are minimized by their high resistivity relative to metals.

4.3. Thin-Film Magnetic Metallic Media. Advanced magnetic recording media are in the form of thin films. The metallic media are typically sputtered films having carbon overcoats for protection. Cobalt-based alloys have been developed for use as longitudinal, ie, *c*-axis of the crystalline Co-alloy parallel to the plane of the substrate, magnetic recording media (51) (see COBALT AND COBALT ALLOYS). Magnetic disks are presently fabricated on nickel phosphide [12035-46-0], NiP, coated aluminum alloy disk substrates. An aluminum-base hard disk is illustrated in Figure 5. The NiP is used to provide a polishable surface for the subsequent sputtered Cr-underlayer. For most of the cobalt-based alloys used for recording, the underlayer of chromium is used so as to help in controlling the crystallite orientation (texture) of the film as well as controlling the isolation of the crystallites of the longitudinal recording Co-alloy subsequently deposited on it. Co–Cr–Ta/Cr and Co–Pt–Cr/Cr alloys (42) are being developed for high density longitudinal recording media. Table 3 lists magnetic metals investigated for thin-film devices.

Alloy composition, compositional inhomogeneities in the grains, and deposition parameters including substrate temperature in relation to the isolation of the individual crystallites, ie, the magnetic regions, and properties are all important (Fig. 6). It is generally believed that some isolation of the grains, ie, wider grain boundary regions, is necessary to weaken the exchange coupling among magnetic regions to reduce switching of adjacent crystallites and noise (42). The introduction of nonmagnetic phases at the grain boundaries, by segregation or precipitation for example, should reduce exchange coupling between grains and therefore reduce noise (52) by the formation of a paramagnetic region rich in Cr.

Cobalt–chromium films (20 at.% Cr) exhibiting strong perpendicular anisotropy, ie, hexagonal *c*-axis normal to the substrate surface, have been studied (53). Fifty nanometer films are composed of columnar crystallites and the domain size was found to be a few structural columns in diameter. Magnetization reversal was shown to occur by domain rotation in thick films. Thinner (ca 10-nm thick) films do not show the columnar crystallite morphology. These exhibit well-defined 180° domain walls and magnetization reversal occurs by domain wall motion. Material of intermediate thickness exhibits a microstructure which shows in-plane (longitudinal) and out-of-plane (perpendicular) components. Magnetization reversal by domain rotation in the columnar grains leads to high recording density.

Reference 37 provides excellent overviews of metallic films, materials science of thin magnetic recording materials, and the potential technological significance.

4.4. Magnetooptic Materials. The application of magnetooptic effects to optical memory systems, such as for laser beam writing and magnetooptic read, has been the subject of much research. Magnetooptic storage media offer the potential of storing over 120 $Mbit/cm^2$ of information without contact of the read/write head which would thus be very competitive to floppy disks and tape.

Memory systems based on laser writing and reading through the interaction of electromagnetic radiation, either through reflection utilizing the Kerr effect or by transmission utilizing the Faraday effect, have begun to appear in the marketplace. As of this writing, recording systems utilizing disks of 90 and 130 mm in diameter are appearing. Recording depends on creating regions of reverse magnetization in films which exhibit uniaxial magnetic anisotropy normal to the film and a relatively low (100–200°C) Curie temperature which results in a strong temperature dependence of coercivity and magnetization. Coercivities of the order of 80 kA/m (1000 Oe) are required at room temperature and about 8 kA/m (100 Oe) at 200°C. Thus the local heating of a submicrometer laser beam impinging on the film can easily heat a submicrometer region near or above the Curie temperature. The demagnetizing field of adjacent material causes a region of reverse magnetization which persists to room temperature. The recorded information can be read using the magnetooptic Kerr effect. Erasure of the recorded information is accomplished by irradiation of the film (heating) with the bias magnetic field in the opposite direction.

The magnetic storage media being employed are ternary amorphous alloys (Table 3) composed of the rare-earth elements gadolinium, Gd, and terbium, Tb, with Fe and Co for use in the near infrared. These materials are compatible with GaAs-based lasers (37). These alloys are ferrimagnetic, ie, the atomic moments of the rare-earth atoms, owing to the 4*f* electrons, couple antiferromagnetically to the atomic moments of Fe and Co resulting from their 3*d* electrons. This negative exchange interaction gives rise to ferrimagnetic behavior resulting in a small net moment or magnetization which is temperature dependent. There is a compensation temperature where the 4*f* and 3*d* magnetizations are equal but opposite in sign and cancel, resulting in a nonmagnetic material. This compensation temperature is below room temperature, but above this temperature the 3*d*-electron magnetization is smaller than that which would be exhibited if no rare-earth atoms were in the alloy. Thus the magnetization of interest to magnetooptic recording can be tailored based on the above negative exchange interaction that occurs between some of the rare-earth and Fe-group atoms.

The rare-earth (R) garnets, $R_3Fe_5O_{12}$, which are ferrimagnetic, are being investigated for magnetooptic recording. Atomic substitutions for the trivalent R and Fe atoms result in garnets having the required high room temperature coercivity and Curie temperature range (150–260°C). An example is $Bi_2DyFe_{3.6}Al_{1.2}O_{12}$ referred to as a Bi-substituted garnet (54). Films of several garnets in the system $(GdPrTmBi)_3(Fe,Ga)_5O_{12}$ have been proposed for use in magnetooptic read heads (55). Further work on garnets and ultrathin Pt/Co or Pd/Co multilayers containing Pt or Pd of about 1-nm thick and Co layers about

0.35-nm thick is required to establish their possible use for magnetooptic recording (37,43,44).

Amorphous single-domain CoTaZr cores having Al_2O_3 interlayers where the CoTaZr thickness is from 0.23–0.9 μm, depending on the number of layers, and Al_2O_3 is 0.01-μm thick, were evaluated for use as thin-film heads (46). This material combination is attractive for low noise heads operating at frequencies up to 40 MHz (46). Similarly, the read/write characteristics of laminated cores consisting of four layers made of Fe–Ta–N films 0.5-μm thick separated by 0.1-μm Al_2O_3 layers are characterized by high magnetic saturation and permeability and are attractive for high definition television (HDTV) (47).

Magnetooptical recording in sputtered Co/Pt multilayers (0.4 nm Co–1.4 nm Pt) and $Gd_{17}Tb_8Fe_{75}$ disks were evaluated at wavelengths of 820, 647, and 458 nm, corresponding to AlGaAs, krypton, and argon lasers, respectively. At 458 nm, Co/Pt performed 3 dB better than GdTbFe. This was attributed to the higher Kerr signal exhibited by Co/Pt, low noise level, and quality of the written domain structure (56).

Synthetic magnetic superlattices can be considered important new materials. The perpendicular anisotropy developed by ultrathin layered superlattices, such as Co/Pt and Co/Pd, in contrast to the more usual tendency for the preferred direction of the magnetization to be in the film plane (shape anisotropy) because of lower magnetostatic energy, appears to arise from the interfacial areas of the composite. The magnetic anisotropy energy was shown to be proportional to the reciprocal of the thickness of the Co-layers and perhaps is a consequence of the atomic disorder at the interfaces. The surface area-to-volume ratio is large and thus should dominate the magnetic anisotropy below a certain thickness (57–59).

4.5. Magnetic Superlattices. The discovery in the late 1980s of giant magnetoresistance (GMR) in antiferromagnetically coupled Fe/Cr superlattices (60,61) stimulated great interest. Properties of metallic superlattices consisting of thin alternate single-crystal layers of different magnetic materials as well as alternate layers of magnetic and nonmagnetic materials were examined.

Epitaxically oriented single-crystal layers of Fe and Cr have been prepared by MBE on exceptionally clean (001) GaAs single-crystal substrates (60,61). The notation for one individual bilayer is ((001)Fe/Cr(001)). The individual layer thickness ranges from 0.9 to 9 nm and the total number of bilayers in a single film is around 30. Notation for a complete superlattice of 30 bilayers would be $(Fe\ 3\ nm/Cr\ 1.2\ nm)_{30}$. Chromium, in bulk form, is antiferromagnetic. At low temperatures and in zero-applied field, the magnetization behavior of each successive layer is antiparallel and the electrical resistance of the film is high (Fig. 7**a**). When a magnetic field is applied parallel to the layers and is sufficient to overcome the antiparallel arrangement of the layer magnetizations (Fig. 7**b**), the electrical resistance of the film begins to decrease. When this occurs, the film is said to exhibit a negative magnetoresistance. The complete switching fields (H_S), for a constant negative magnetoresistance, for several Fe/Cr superlattices at 4.2 K, are shown in Figures 8 and 9. H_s for the saturation of magnetoresistance is a function both of composition of the individual layers and the number of bilayers. There is also an anisotropy in the magnetoresistance as illustrated in Figure 9 (60).

Magnetoresistive recording heads offer much more sensitivity than inductive heads (63) and there is strong evidence as of this writing (ca 1994) that such heads will be used exclusively by the year 2000. The trend in the development of head materials is toward thin-film media. Although Permalloy films ($Ni_{18}Fe_{19}$) are used for magnetoresistive sensors, the change in resistance is only about 2.5%. Higher magnetoresistive materials are needed. The Fe/Cr GMR system requires large (ca 1 T) switching fields to align the magnetization in the layers (60,61). Weaker interlayer interactions are needed to obtain the desired resistivity change at low fields and at room temperature. Table 4 summarizes some of the work along these lines. Theoretical discussions of the microscopic origin of GMR can be found in References (70–74). Materials-related aspects of multilayered materials are summarized in References 75 and 76.

4.6. Magnetic Fluids. Magnetic fluids are stable colloidal suspensions of ferromagnetic particles, such as Fe_3O_4 and of subdomain size (ca 10 nm) in aqueous or organic bases (77,78). The fluid behaves as a homogeneous Newtonian liquid and reacts to a magnetic field. These materials are used in bearings, rotary-shaft seals, and feedthroughs (see BEARING MATERIALS). Other possible applications, eg, as jet inks and for float separation, have been studied (79) (see SEPARATION, MAGNETIC SEPARATION). Fluid properties, such as magnetic moment, viscosity, and density, can be tailored for various applications if the proper choice of particle concentration, composition and size, particle coatings, and liquid base is made.

BIBLIOGRAPHY

"Magnetic Materials, Thin Film" in *ECT* 3rd ed., Vol. 14, pp. 686–707, by J. H. Wernick and G. Y. Chin, Bell Laboratories.

CITED PUBLICATIONS

1. B. D. Cullity, *Introduction to Magnetic Materials*, Addison-Wesley, Reading, Mass., 1972.
2. M. Prutton, *Ferromagnetic Films*, Butterworths, London, 1964.
3. J. F. Freedman, *IEEE Trans. Magn.* **MAG-5**, 752 (1969).
4. E. W. Pugh, in G. Haas, ed., *Physics of Thin Films*, Vol. **I**, Academic Press, Inc., New York, 1963.
5. R. E. Thun, *Rev. Elec. Comm. Lab.* **25**, 209 (Mar./Apr. 1977).
6. E. Pugh and T. O. Mohr, *Thin Films: Properties of Ferromagnetic Films*, ASM, Metals Park, Ohio, 1963, Chapt. 7.
7. T. Serikawa, in Ref. 5.
8. B. L. Flur, in *Physics of Thin Films*, Vol. **3**, Academic Press, Inc., New York, 1966.
9. R. Glang, in L. I. Maissel and R. Glang, eds., *Handbook of Thin Film Technology*, McGraw-Hill Book Co., Inc., New York, 1970.
10. D. Bouchier and co-workers, *J. Appl. Phys.* **49**, 5896 (1978).
11. L. I. Maissel and P. M. Schaible, *J. Appl. Phys.* **36**, 237 (1965).
12. H. C. Theurer and J. J. Hauser, *Trans. AIME* **233**, 588 (1965).
13. L. I. Maissel, in Ref. 8.

14. J. L. Vossen and J. J. O'Neill, Jr., *RCA Rev*., 149 (June 1968).
15. G. N. Jackson, *Thin Solid Films* **5**, 209 (1970).
16. A. M. Marsh and co-workers, *Appl. Phys. Lett*. **62**(9), 952 (Mar. 1, 1993).
17. R. C. Baumann, R. A. Rost, and T. A. Robson, *Mater. Res. Soc. Symp. Proc*. **200**, 25 (1990).
18. D. Roy and S. B. Kruopanidhi, *Appl. Phys. Lett*. **62**(10), 1056 (Mar. 8, 1993).
19. A. Y. Cho, *J. Appl. Physics* **41**, 2780 (1970).
20. M. B. Panish, *J. Electrochem. Soc*. **127**(12), 2729 (1980).
21. H. M. Manasvet and W. I. Simpson, *J. Electrochem*. **116**, 1725 (1969).
22. H. M. Manasvet, *J. Crystal Growth* **55**, 1 (1981).
23. G. B. Stringfellow, *J. Crystal Growth* **68**, 111–122 (1984).
24. J. E. Mee and co-workers, *IEEE Trans. Magn*. **MAG-5**, 717 (1969).
25. J. W. Nielsen, *Met. Trans*. **2**, 625 (1971).
26. I. W. Wolf, *J. Appl. Phys*. **33**, 1152 (1962).
27. R. Girard, *J. Appl. Phys*. **38**, 1423 (1967).
28. D. J. Wollons, *Introduction to Digital Computer Design*, McGraw-Hill Book Co., Inc., London, 1972.
29. E. A. Giess and R. Ghez, in *Epitaxial Growth*, Part A, Academic Press, Inc., New York, 1974, p. 183.
30. A. R. Corradi, *IEEE Trans. Magn*. **MAG. 14**, 655 (1978).
31. C. D. Mee, *The Physics of Magnetic Recording*, North Holland, Amsterdam, 1963; *Inst. Elec. Electron. Engrs. Trans. Commun. Electron*., 399 (1964).
32. R. P. Hunt, *IEEE Trans. Magn*. **MAG-7**, 150 (1975).
33. R. W. Keyes, *Comments Solid State Phys*. **5**, 97 (1973).
34. R. C. Sherwood and co-workers, *J. Appl. Phys*. **42**, 1704 (1971).
35. E. Sawatzky and G. B. Street, *J. Appl. Phys*. **44**, 1789 (1973).
36. C. H. Bajorek and R. J. Kobliska, *IBM J. Res. Dev*., 271 (May 1976).
37. M. H. Kryder, *Thin Solid Films* **216**, 174 (1992); S. D. Bader, *Proc. IEEE* **78**(6), 909 (1990).
38. D. Raasch, *IEEE Trans. Magn*. **29**(1), 34 (1993).
39. N. Heiman, R. D. Hempstead, and N. Kazama, *J. Appl. Phys*. **49**, 5663 (1978).
40. Y. Maeda and M. Takahashi, *J. Appl. Phys*. **68**, 4751 (1990).
41. Y. Maeda and M. Asahi, *J. Appl. Phys*. **61**, 1972 (1987).
42. Y. Maeda and K. Takei, *IEEE Trans. Magn*. **27**(6), 472 (1991).
43. H. Yamane, Y. Maeno, and M. Kobayashi, *Appl. Phys. Lett*. **62**, 1562 (1993).
44. F. J. A. Den Broeder and co-workers, *Appl. Physics* **A**, 507 (1989).
45. B. M. Lairson and co-workers, *Appl. Phys. Lett*. **62**, 639 (1993).
46. R. Arai and co-workers, *IEEE Trans. Magn*. **28**(5), 2115 (1992).
47. T. Okumura and co-workers, *IEEE Trans. Magn*. **28**(5), 2121 (1992).
48. F. J. A. Den Broeder and co-workers, *Appl. Phys. Lett*. **61**(12), 1468 (1992).
49. F. J. A. Den Broeder and co-workers, *Phys. Rev. Lett*. **60**(26), 2769 (1988).
50. D. Weller and co-workers, *Appl. Phys. Lett*. **61**(22), 2726 (1992); P. F. Garcia and Z. G. Li, *Appl. Phys. Comm*. **11**, 531 (1992).
51. D. E. Laughlin and B. W. Wong, *IEEE Trans. Magn*. **27**, 4713 (1991).
52. T. Chen and T. Yamashita, *IEEE Trans. Magn*. **24**, 2700 (1988).
53. B. G. Demczyk, *IEEE Trans. Magn*. **28**(2), 998 (1992).
54. K. Shono and co-workers, *Mater. Res. Symp. Proc*. **150**, 131 (1989).
55. B. Ferrand and co-workers, *IEEE Trans. Magn*. **24**, 2563 (1988).
56. W. B. Zeper and co-workers, *IEEE Trans. Magn*. **28**(5), 2503 (1992).
57. H. J. G. Draaisma, W. J. M. de Jonge, and F. J. A. de Broeder, *J. Magn. and Magn. Mat*. **66**, 351 (1987).
58. L. Neel, *J. Phys. Rad*. **15**, 225 (1954).

59. F. Hakkens and co-workers, *J. Mater. Res*. **8**(5), 1019 (1993).
60. M. N. Baibich and co-workers, *Phys. Rev. Lett*. **61**, 2472 (1988).
61. G. Binasch and co-workers, *Phys. Rev*. **B39**, 4828 (1989).
62. L. M. Falicov, *Physics Today*, 46 (Oct. 1992).
63. C. Tsang, *J. Appl. Phys*. **55**, 2226 (1984).
64. D. H. Mosch and co-workers, *J. Magn. Magn. Mat*. **94**, L1 (1991).
65. K. Inomata and Y. Saito, *Appl. Phys. Lett*. **61**(6), 726 (1992).
66. S. S. P. Parkin, *Appl. Phys. Lett*. **61**(11), 1358 (1992); *Phys. Rev. Lett*. **71**, 1641 (1993); *Mat. Lett*. **20**, 1 (1994).
67. T. Valet and co-workers, *Appl. Phys. Lett*. **61**(26), 3187 (1992).
68. B. Dieny and co-workers, *Phys. Rev*. **B43**, 1297 (1991).
69. L. F. Schelp and co-workers, *Appl. Phys. Lett*. **61**(15), 1858 (1992).
70. R. L. White, *IEEE Trans. Magn*. **28**(5), 2482 (1992).
71. D. M. Edwards, J. Mathon, and R. B. Muniz, *IEEE Trans. Magn*. **27**, 3548 (1991).
72. R. E. Camley and J. Barnas, *Phys. Rev. Lett*., 63 (1989).
73. J. Barnas and co-workers, *Phys. Rev*. **B42**, 8110 (1990).
74. P. Grünburg and co-workers, *J. Magn. Magn. Mater*. **93**, 58 (1991).
75. *Mat. Res. Soc. Bull*. **15**(2), (Feb. 1990).
76. *Mat. Res. Soc. Bull*. **15**(3), (Mar. 1990).
77. R. E. Rosensweig, *J. Sci. Technol*. **48** (July 1966).
78. S. W. Charles and J. Poppewell, in E. P. Wohlfarth, ed., *Ferromagnetic Materials*, North Holland, Amsterdam, 1980.
79. *IEEE Trans. Magn*. **16** (Mar. 1980).

GENERAL REFERENCES

M. H. Kryder, "Data Storage in 2000: Trends in Data Storage Technologies," *IEEE Trans. Magn*. **25**(6), 4358 (1989).
M. P. Sharrock, "Particulate Magnetic Recording Media: A Review," *IEEE Trans. Magn*. **25**(6), 4374 (1989).
P. Hansen and H. Heitmann, "Media for Erasable Magnetooptic Recording. *IEEE Trans. Mag*. **25**(6).
J. M. E. Harper, "Ion Beam Techniques in J. M. E. Harper," *Solid State Technol*., 129 (Apr. 1987).
O. Kohmoto, "Recent Developments of Thin Film Materials for Magnetic Heads," *IEEE Trans. Magn*. **27**(4), 3640 (1991).
T. Kunieda, K. Shinohara, and A. Tomago, "Metal Evaporated Video Tape," *Proc. IERE* **59**, 37 (1984).
B. Heirich and J. A. C. Bland, eds., *Ultrathin Magnetic Structures*, Springer, Berlin, 1994.

JACK WERNICK

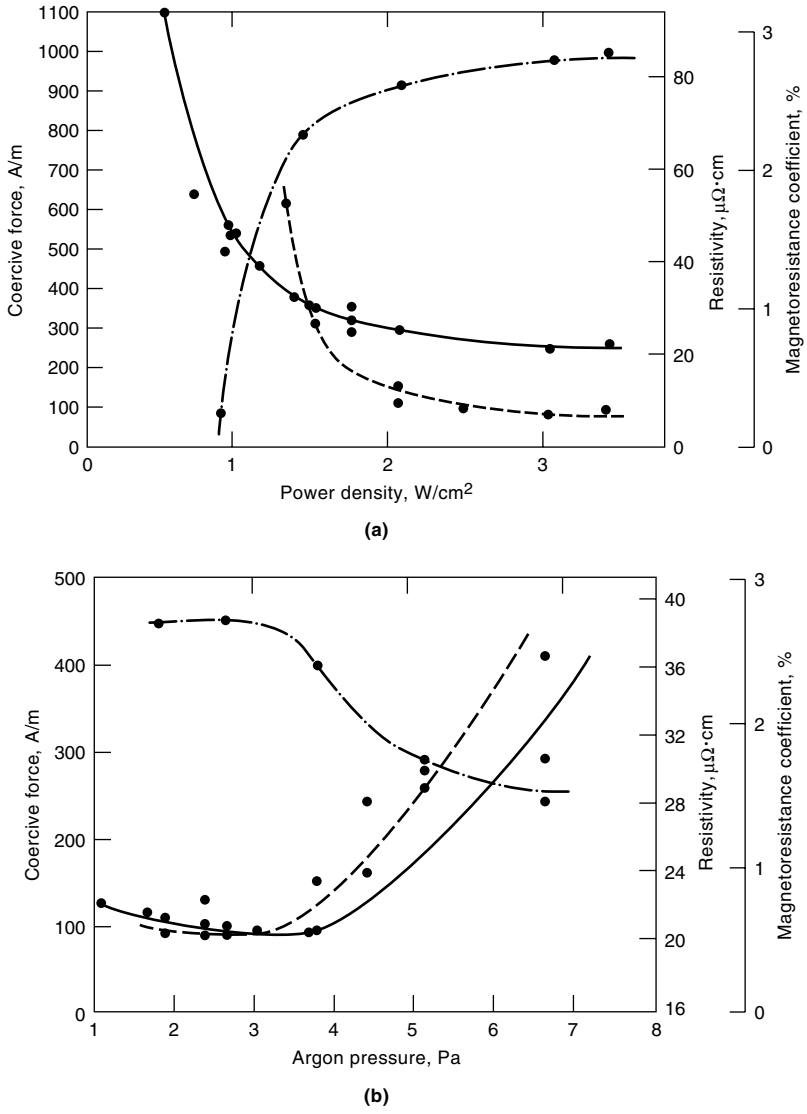

Fig. 1. The effect of (– – –) coercive force, (—) resistivity, and ([[art1]]) magnetoresistance coefficient for Permalloy films (**a**) at a constant argon pressure of 2.9 Pa (2.2×10^{-2} mm Hg) and (**b**) argon pressure at a constant power density of 3 W/cm^2 (7). To convert A/m to Oe, divide by 79.58; to convert Pa to mm Hg, divide by 133.3.

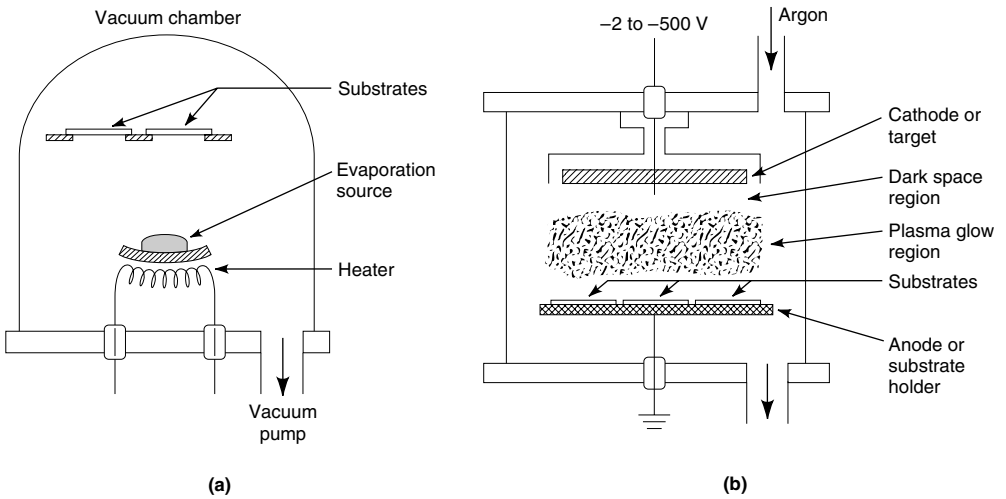

Fig. 2. Simple schematic representation of (**a**) vacuum evaporation and (**b**) cathodic sputtering.

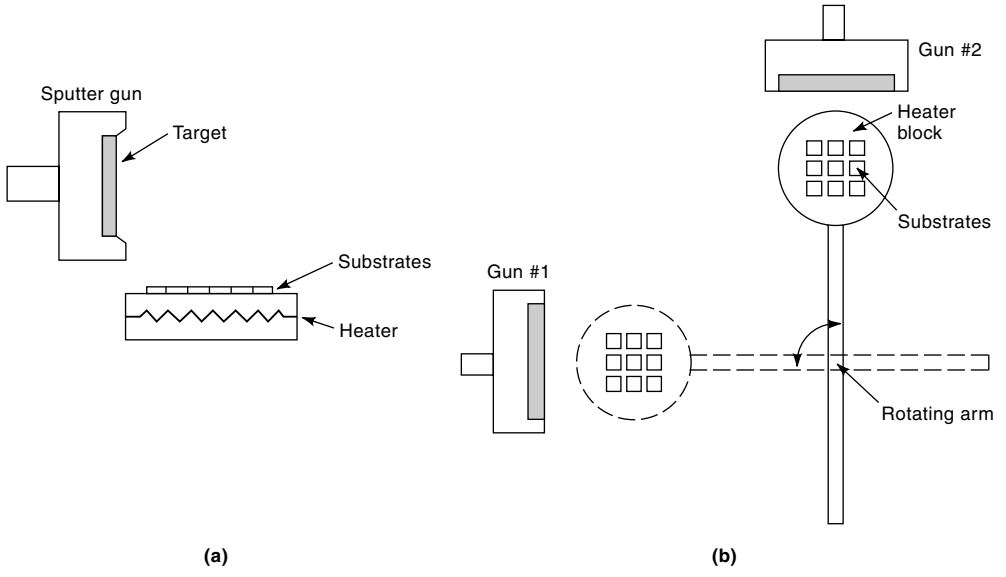

Fig. 3. Schematic configuration of (**a**) the 90° off-axis sputtering technique and (**b**) the system used to prepare multilayers.

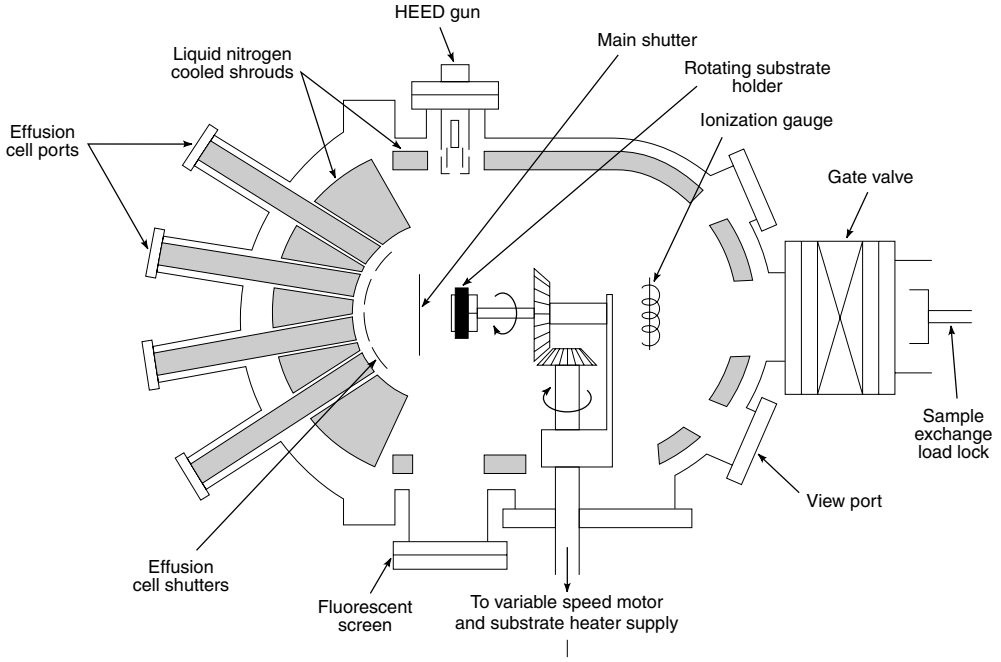

Fig. 4. Schematic of a high vacuum molecular beam epitaxy (MBE) chamber containing four effusion (Knudsen) cells. Also shown is a high energy electron diffraction (HEED) unit for monitoring the deposition as it occurs.

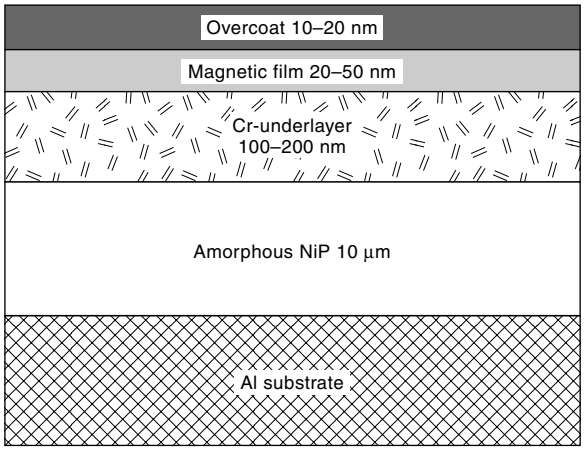

Fig. 5. Schematic drawing of the various layers in a hard disk (51).

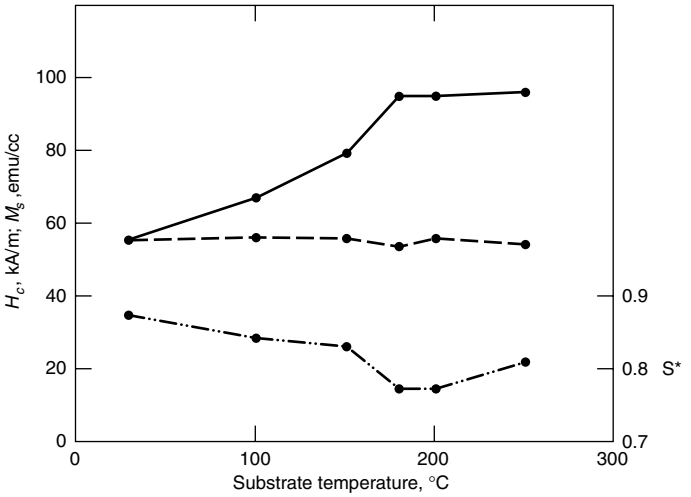

Fig. 6. Changes in (———) coercive force, H_c, (– – –) saturation magnetization M_s, and (—··—) coercive squareness ratio, S^*, of Co–Cr–Ta/Cr films deposited on Cr-underlayers on polymide substrates for longitudinal recording as a function of substrate temperature; d-c magnetron sputtering was used (42). To convert kA/m to Oe, divide by 7.958×10^{-2}.

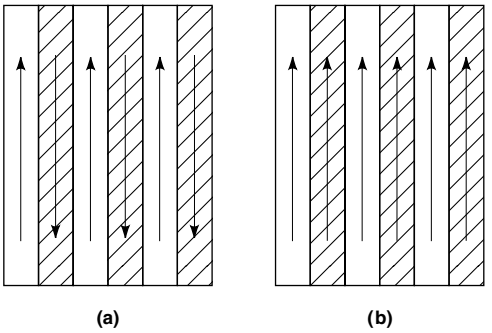

Fig. 7. Schematic representation of an antiferromagnetic magnetic multilayer superlattice in (**a**) zero-applied field ($H = 0$) at 4.2 K and (**b**) in an applied field H_s sufficient to establish saturated negative magnetoresistance (62).

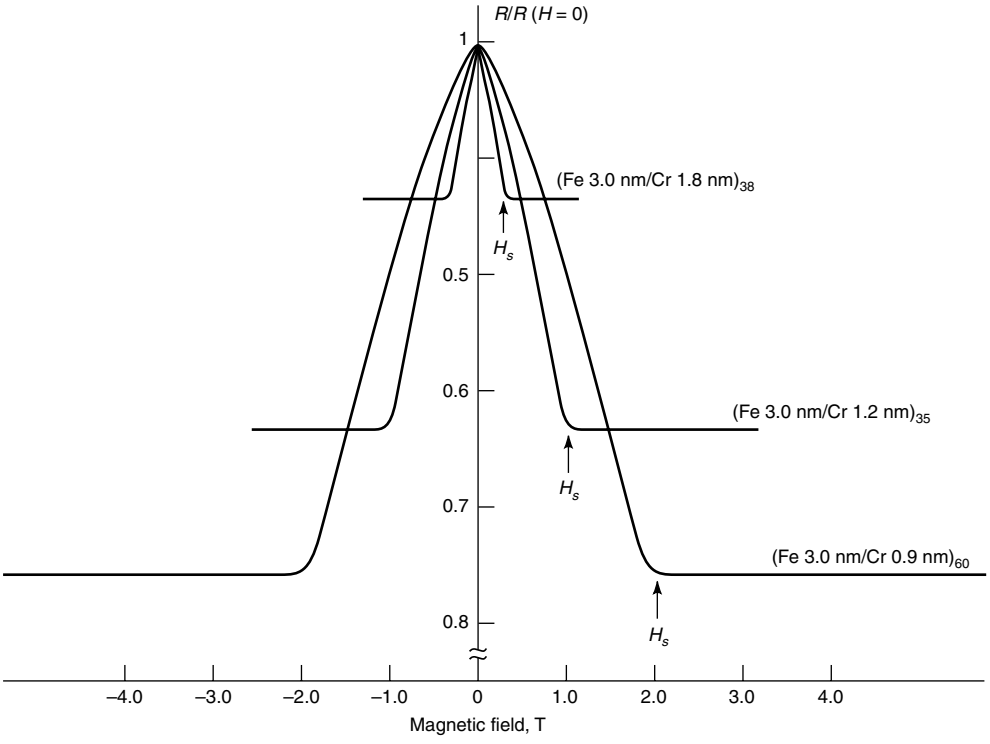

Fig. 8. Giant negative magnetoresistance $R/R(H = 0)$ behavior of three Fe/Cr superlattices as a function of applied field at 4.2 K showing the value of the complete switching field, H_s, for each lattice. The current and the applied field are along the (110) direction in the plane of the layers (60). To convert T to G, multiply by 10^4.

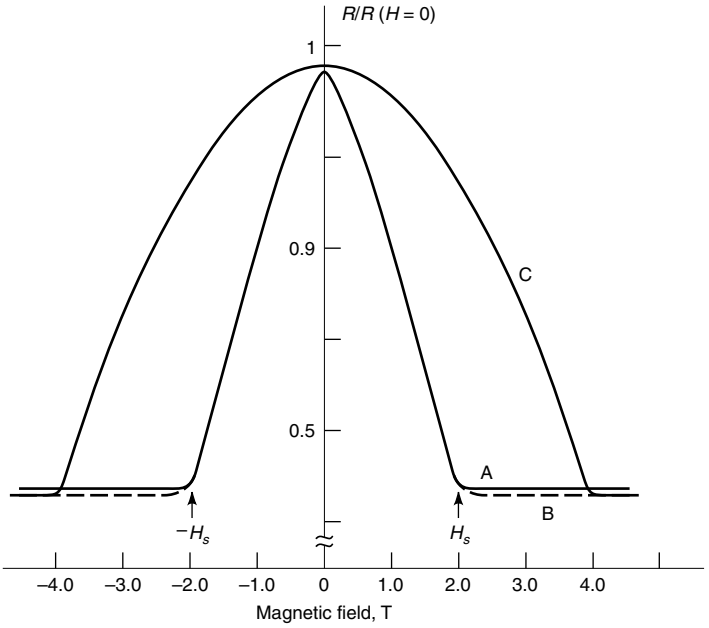

Fig. 9. Effect on (Fe 3.0 nm/Cr 0.9 nm)$_{40}$ magnetoresistance, $R/R(H = 0)$, of changing the direction of the applied field relative to the current direction of [110] in the plane, where A represents an applied field in the layer plane along the current direction; B, (–) the applied field in the layer plane, but directed perpendicular to the current direction; and C, the applied field perpendicular to the layer plane (60).

Table 1. **Magnetic Properties of Sputtered Films**[a]

	No bias			Negative bias[b]		
Rate, nm/s	H_c, A/cm[c]	H_k, A/cm[c]	$\Delta\alpha$	H_c, A/cm[c]	H_k, A/cm[c]	$\Delta\alpha$
2.70	1.51	2.47	2.0°	1.83	1.99	6.2°
1.65	1.99	3.10	2.5°	1.19	2.63	2.8°
1.20	2.63	3.42	3.6°	1.83	3.10	2.2°
0.75	5.41	4.78	3.9°	1.59	2.87	3.3°
0.40	12.74			1.19	3.42	1.3°

[a] Ref. 8.
[b] Bias of −100 V.
[c] To convert A/cm to Oe, divide by 0.7958.

Table 2. **Magnetic Properties of Common Magnetic Recording Media**

Material	B_r, T[a]	H_c, kA/m[b]
γ-Fe_2O_3	0.11	26
Fe_2O_3–Fe_3O_4	0.15	37
Co–γ-Fe_2O_3	0.15	52
CrO_2	0.15	45
$BaFe_{12}O_{19}$	0.12	64
Fe	0.30	120

[a] To convert T to G, multiply by 10^4

[b] To convert kA/m to Oe, divide by 7.958×10^{-2}

Table 3. **Magnetic Metals Investigated For Thin-Film Devices**

Material	Composition, wt %	Application	Reference
iron		MR	31
iron–nickel alloys	Permalloys	MR	31
		MD, T, RH	32
cobalt–nickel	82 Co, 18 Ni		
cobalt–phosphorus	98 Co, 2 P	R	31
cobalt–nickel–phosphorus	75 Co, 23 Ni, 2 P	R	31
iron–nickel–chromium	76 Fe, 12 Ni, 12 Cr 74 Fe, 8 Ni, 18 Cr		
Vicalloy II	13 V, 35 Fe, 52 Co	R	31
Cunife I	60 Cu, 20 Ni, 20 Fe	R	31
Cunife II	50 Cu, 20 Ni, 27.5 Fe, 2.5 Co	R	31
Cunico I	50 Cu, 21 Ni, 29 Co	R	31
Cunico II	35 Cu, 24 Ni, 41 Co	R	31
manganese bismuth (1:1)		TH	33
manganese aluminum germanide		TH	34
manganese gallium germanide		TH	35
Sendust alloy	85 Fe, 9.6 Si, 5.4 Al	TS, 12-μm films, RH,	35
RCo(Fe) amorphous alloys	variable	MRM	(36–38)
Co–Fe–Cr–P–C–B amorphous alloys	variable	SMB, $H_c < 8$ A/m	39
Co–Cr	18–22 Cr	PR, LR	(40, 41)
Co–Cr–Ta/Cr, Co–Pt–Cr/Cr		LR	42
Pt/Co or Pd/Co multilayers	ultrathin alternating layers	MRM	(37, 43, 44)
Pt/Fe epitaxial multilayers	3 nm Pt/2.3 nm Fe	MRM, PR	45
CoTa–Zr amorphous multilayers on Al_2O_3 separators	variable	HFRH	46
FeTaN multilayers on Al_2O_3	0.5 μm alloy/0.1 μm Al_2O_3	RH/HDTV	47
Co/Ni multilayers	variable	MRM, PR	48
Co/Au multilayers	variable	PR	49
$Co_{1-x}Pt_x$ multilayers	$x = 0.45 - 0.9$	PA, MRM	50

[a] MR = magnetic recording; MD = magnetoresistive detectors; T = transducers; RM = recording heads; R = recording; TH = thermomagnetic or Curie-point writing; TS = tetrode sputtering; MRM = magnetooptic recording media or magnetooptical recording; SMB = soft magnetic behavior; PR = perpendicular recording; LR = longitudinal recording; HFRH = high frequency recording heads; RH/HDTV = recording heads for high definition television; and Pa = perpendicular perpendicular anisotropy.

[b] The CAS Registry Number is [12010-50-3].

[c] The CAS Registry Number is [12042-22-7].

[d] The CAS Registry Number is [37195-97-4].

[e] Where R = Gd or Tb.

[f] 8 A/m = 0.10 Oe.

Table 4. **Magnetic Superlattices Exhibiting GMR**

Material system	Multilayer information	Result[a,b,c]	Reference
Fe/Cr	variable ((001) Fe/Cr(001))$_n$, 0.9–9.0-nm single-crystal layer thick-ness on single-crystal GaAs	resistivity lowered by as much as a factor of two at 4.2 K and switching fields of the order of 1 T are required	(60,61)
Co/Cu	variable	strong antiparallel cou-pling through the non-ferromag-netic copper; high ($>$ 800 kA/m) fields required to change antiferromag-netic spin structure into a ferromagnetic one	(61,64)
Co–Fe/Cu	1.0 nm Co_9Fe/1.0 nm Cu ion-beam sputtering on MgO(110) sub-strates	Co–Fe/Cu grew having inplane uniaxial aniso-tropy and easy axis parallel to the cube direction in the MgO(110) plane; satu-ration field (240 kA/m) at room temperature for GMR = 45%	65
Ni,Fe/Cu	$Ni_{81}Fe_{19}$/Cu/Co	GMR dramatically en-hanced by presence of the thin Cu layer; mag-netoresistance of more than 17% for field changes of $\pm$8 kA/m at room temperature	66
Ni,Fe/Cu/Co	[$Ni_{80}Fe_{20}$/Cu/Co/Cu] r-f diode sput-tering on Si(100) single-crystal wafers at room temperature	resistance changes as large as 70% within a few tens of amperes per meter	67
NiFe/Cu/NiFe/FeMn		resistance changes of 3–4% in fields of 40–800 A/m	68
Co/Ag	Co(15 nm)/Ag(6.0 nm) electon-beam evapora-tion on top of a 5.0-nm Cr buffer layer on Si(111) substrates	interface roughness ap-pears to be important in under-standing the connection between GMR and antiferromag-netic coupling	69

[a] To convert T to G, multiply by 10^4.
[b] To convert kA/m to Oe, divide by 7.958×10^{-2}.
[c] GMR = giant magnetoresistance.